

Statistics of Velocity Gradients in Two-Dimensional Navier-Stokes and Ocean Turbulence

Norbert Schorghofer

Department of Earth, Atmospheric, and Planetary Sciences,
Massachusetts Institute of Technology, Cambridge, MA 02139

Sarah T. Gille

Department of Earth System Science,
University of California, Irvine, CA 92697-3100

February 20, 2019

Abstract

We report measurements for the statistics of velocity gradients in upper ocean turbulence and in simulations of the two-dimensional Navier-Stokes equations. Ocean data are derived from TOPEX satellite altimeter measurements. The simulations use rapid forcing on large scales. Probability density functions of velocity and transverse velocity gradients closely agree between the two kinds of turbulence. In the simulations, longitudinal and transverse derivatives have different probability density functions, in contrast to what is found for decaying two-dimensional turbulence.

Statistical properties of turbulent flows, such as probability density functions (pdfs), are important for characterizing turbulence. For instance, velocity gradients are directly related to the velocity correlation across small separations and to the total energy dissipation in the fluid [1]. The statistics of velocity gradients have been successfully understood to result from well-separated vortices [2, 3], if the two-dimensional turbulence is in the late stages of decay. A qualitatively different behavior is found from numerical simulations of steady two-dimensional turbulence. This study is further devoted to evaluating statistical properties of turbulence, as observed in recent satellite measurements of the upper ocean. Statistics of observed phenomena are compared with corresponding statistics for the forced two-dimensional

Navier-Stokes equations. Our results show that, in contrast with unforced decaying turbulence, simple forced two-dimensional Navier-Stokes equations agree with ocean observations.

For this study, ocean velocities are derived from altimeter data collected by the TOPEX/POSEIDON satellite, which performs repeated measurements of the height η of the ocean surface. The geostrophic relation, $v_x = (g/f)\partial\eta/\partial y$, yields the velocity component perpendicular to the satellite ground track. Surface geostrophic velocities are characteristic of sub-surface flow in the ocean [4]. This geostrophic flow is typically well-represented by two-dimensional shallow-water equations and resembles two-dimensional turbulence [5, 6]. The derivative along the satellite track, $\partial_y v_x$, yields the transverse velocity gradient; the cross-track, or longitudinal, derivative cannot be determined. Higher order derivatives are increasingly noisy.

We compare observed oceanic pdfs with simulations of the two-dimensional Navier-Stokes flow for an isotropic, homogeneous, and statistically stationary situation. Simulations use a conventional pseudo-spectral method and genuine second-order dissipation. Rapidly varying (white-in-time) forcing is applied on large scales. This forcing resembles wind forcing of the ocean, which varies rapidly in time but slowly in space [7, 8]. Results were obtained on a 1024×1024 grid with long time averaging. Further details about the numerics and resulting velocity pdfs are described elsewhere [9, 10].

Earlier results have shown that velocities typically have Gaussian distributions within small regions of the ocean. When satellite data from the global ocean were combined, the resulting pdfs were non-Gaussian, due to regional variations in velocity variance [11, 12]. When velocities were normalized by their local variances, the pdfs were Gaussian [12], at least for well-sampled velocities within 3 standard deviations of the mean. Similar results were obtained for subsurface floats deployed in the North Atlantic Ocean, although analysis for velocities more than three standard deviations from the mean indicated non-Gaussian tails [13]. In this study, we specifically normalize velocities and velocity gradients by their local variances before computing pdfs and other statistics.

Velocity pdfs are Gaussian, as a number of recent studies have shown both for simulated flows [2, 9, 14] and for ocean observations [11, 12, 13]. Since Gaussian distributions are ubiquitous, this commonality is not surprising and could be purely coincidental. Velocity gradients are not as thoroughly studied as velocity pdfs. Previous studies suggest, however, that gradients do not exhibit a universal pdf: idealized models of point vortices predict a Cauchy distribution [2, 3, 15, 16], in agreement with results from decaying two-dimensional turbulence [2]. In contrast, pdfs of ocean surface velocity gradients are observed to have more rapidly decaying tails [11].

Figure 1 shows velocity gradient pdfs derived from ocean observations and simulations. The solid line indicates the pdf of normalized velocity gradient data derived from global satellite altimetry. To determine the oceanic pdf, velocity gradient data drawn from latitudes

between 10° and 60°N and between 10° and 60°S are sorted geographically into 2.5° by 2.5° boxes. Data near the equator are omitted because the geostrophic relationship is weak at low latitudes. The standard deviation of gradients in each latitude-longitude box varies from $1.4 \times 10^{-5} \text{ s}^{-1}$ near 60° latitude up to $6.4 \times 10^{-5} \text{ s}^{-1}$ near 10° latitude, with a median value of $1.9 \times 10^{-5} \text{ s}^{-1}$. To compensate for this geographic variation, gradients are normalized to have unit standard deviation in each box, and then the pdf is computed from all of the normalized gradient data. For comparison, we also normalized our pdfs using the mean absolute value of the velocity gradient; this did not diminish the strong tails of the gradient pdf.

The dashed line in Figure 1 represents the transverse velocity gradient pdf from two-dimensional Navier–Stokes turbulence. The dotted line is a Gaussian. The tails contribute noticeably to the standard deviation of the pdf, and therefore the Gaussian is fitted to the data without requiring unit area and unit standard deviation. This is necessary to make the Gaussian closely approximate the central part of the pdf. Both the simulated and observed gradient pdfs appear Gaussian for small velocity gradients, up to about one standard deviation. For large gradients they decay significantly more slowly than do Gaussian tails but faster than the Cauchy distribution, $c/[\pi(c^2 + x^2)]$, found in simulations of decaying turbulence [2, 3]. There is good agreement between observed and simulated pdfs up to even the largest fluctuations measured in the simulation.

Kurtosis serves as quantitative characterization of the shape of the pdf. In the simulation results, the velocity gradient pdf has a kurtosis of 4.7, indicating clear deviation from Gaussianity. If the observed ocean pdf is terminated beyond the extent of the simulated one, at about four and a half standard deviations, its kurtosis is also 4.7. However, the contribution of the tails to the fourth moment is substantial, and the full oceanic pdf has a considerably higher kurtosis of 9.1. Since satellite observations are subject to high measurement noise, this high kurtosis may simply be a manifestation of the excess outliers due to noise. The close agreement between transverse velocity gradient pdfs suggests that ocean geostrophic flows are well represented by the forced Navier–Stokes simulations.

The difference in the length of the tails in Figure 1 indicates the vast difference in the Reynolds number for the ocean and the simulation. The basic simulations had a large-scale Reynolds number on the order of 10^4 , while for ocean turbulence a Reynolds number of 10^7 might be typical [17]. Pdfs were also determined for simulations with lower and higher Reynolds numbers, using respectively lower and higher resolutions, but shorter sampling time. There is no significant change in the shape of the pdfs, although these data do not exclude a slow dependence on Reynolds number. The absence of any detectable Reynolds number dependence suggests that the simulation data are close to what they look like at substantially higher Reynolds number and subgrid-scale processes not resolved in the numerical simulation do not alter the results. (On the other hand, statistical properties involving nonlocal quantities, such as structure functions and power spectra, converge more slowly

with Reynolds number, showing a stronger dependence on subgrid-scale phenomena.)

Although only the transverse velocity component can be determined from altimeter data, simulations permit us to examine the longitudinal derivative, $\partial_x v_x$. Figure 2 shows that there is a clear difference between the behavior of the longitudinal and transverse component. The standard deviation of longitudinal fluctuations is about 60% of that for transverse fluctuations. The shape of the pdfs is also different. While the transverse gradients deviate from Gaussianity, the longitudinal gradient pdf more closely approximates a Gaussian. Like the transverse gradient, the longitudinal gradient does not in any way resemble a Cauchy distribution as seen in Figure 2 [9, 11]. The kurtosis of the longitudinal component is 3.5, substantially closer than the transverse component to the Gaussian value of 3, indicating that large longitudinal gradients are much less frequent than large transverse gradients. Since there is a correspondence between the transverse velocity gradient statistics found in the ocean and in the simulation, our results suggest that oceanic longitudinal velocity gradients might be more clearly Gaussian than are transverse velocity gradients.

Several studies of the velocity gradients exist for three-dimensional Navier-Stokes turbulence [18, 19, 20, 21, 22, 23, 24, 25, 26]; Here we consider the two-dimensional case. For the three-dimensional Navier-Stokes equations velocity gradient pdfs decay more slowly than Gaussian pdfs, the transverse (lateral) derivative pdf is asymmetric, and the pdf for transverse and longitudinal derivatives are different from each other. In isotropic and incompressible three-dimensional Navier-Stokes turbulence one can obtain an exact relation between the standard deviation of transverse and longitudinal component: $\langle (\partial_y v_x)^2 \rangle = 2 \langle (\partial_x v_x)^2 \rangle$ [27]. With an analogous calculation we find in the two-dimensional case $\langle (\partial_y v_x)^2 \rangle = 3 \langle (\partial_x v_x)^2 \rangle$, so that the standard deviation for the longitudinal component is $1/\sqrt{3} \approx 58\%$ of that for the transverse component. This agrees with the measured value of 60% in the simulation. Asymmetry of the transverse pdf is related to vortex stretching [1] and therefore absent in two-dimensional Navier-Stokes flow. The corresponding pdf for the ocean is highly symmetric, hence showing no indication of vortex stretching.

Frisch and She [22] have proposed a simple explanation for the form of the tails of the velocity gradient pdf. In their analysis, the gradient is related to the velocity in a nonlinear fashion. Hence, the pdf of the gradient can be related to the pdf of the velocity by a simple change of variable. This transforms the Gaussian velocity pdf into a near-exponential gradient pdf. Intermittency and coherent structures alter this result, but intermittency in forced two-dimensional turbulence is weak. This argument should apply equally to transverse and longitudinal gradients [22]. However, in the two-dimensional simulation the tails have a significantly different form in the transverse and longitudinal directions. Consequently, this explanation is insufficient. Kraichnan [25] has derived the pdf of transverse derivatives, using a closure argument. The kurtosis at asymptotically high Reynolds number is 35/3. The approach is not applicable to two-dimensional Navier-Stokes flow, and it leaves open

the behavior of the longitudinal component. In conclusion, there is no satisfactory theory for the form of the velocity gradient pdf in two-dimensional Navier-Stokes turbulence; in particular theory does not identify why the longitudinal component is closer to Gaussian than the transverse component.

As a complement to gradient pdfs, we also examine the conditional average of the squared velocity gradient as a function of velocity, $\langle (\partial_y v_x)^2 | |v_x|\rangle$. Conditional averages have been used for a variety of purposes in turbulence studies [28, 29, 30]. In particular, Ching [29] derived an expression to link the conditional average of the squared first derivative of a quantity x and the conditional average of the second derivative with the pdf of x itself. We are aware of no previous calculations of the velocity gradient conditioned on the velocity in turbulent flow. The slope of $\langle (\partial_y v_x)^2 | |v_x|\rangle$ is a measure of the correlation between the velocity and the transverse velocity gradient. If there were no correlation between the velocity at a point and the gradient at the same point, the conditional average would be constant for all values of v_x and would be exactly one if velocity gradients were normalized by their standard deviation. In contrast, the graph for the conditional average would have a pronounced slope if gradients and velocities are strongly correlated, as they would be around an isolated vortex for example.

Figure 3 shows the square-root of the measured conditional average together with that for two-dimensional Navier-Stokes. For the ocean, we have normalized both v_x and $\partial_y v_x$ by their standard deviations in each 2.5° by 2.5° geographic box, because both quantities vary spatially. The axes are labeled in units of their respective standard deviations, $\sqrt{\langle v_x^2 \rangle}$, $\sqrt{\langle (\partial_y v_x)^2 \rangle}$, and $\sqrt{\langle (\partial_x v_x)^2 \rangle}$. The correlation between velocity and its gradient is weak, but the gradients tend to be slightly higher when the velocity is large. If oceanic gradients beyond four standard deviations are excluded, which is a fairer comparison with the simulation, the conditional average gets notably closer to one. The longitudinal component of the conditional average exhibits the same behavior as the transverse component (dash-dot line in Figure 3). For both simulations and observations, conditional averages are near one for small velocities, indicating that at low velocity, gradients are almost uncorrelated with velocity. For larger velocities, the gradient increases with velocity both in the ocean and in the simulations.

The real ocean differs from the forced Navier-Stokes system because of the addition of the Coriolis force, stratification, three-dimensional motions, and buoyancy. Although some of these effects may be negligible, the Coriolis force plays a dominant role in ocean flow and is required in order to observe geostrophic velocities using altimetry. However, in the geostrophic relation the Coriolis force is balanced by the hydrostatic pressure variations. Due to this cancellation, the remaining dynamics correspond more closely to flow without Coriolis force and height variations, thus making the statistical properties similar in the simulations and observations. Geostrophic turbulence simulations would shed more light on

this issue.

In conclusion, these simulations of the two-dimensional Navier-Stokes equations are consistent with measurements of upper-ocean turbulence. There is agreement for all available statistical variables: the pdf of velocity, the pdf of transverse velocity gradient, and to a lesser extent their conditional average. Large-scale forcing appears to play an important role in generating the observed turbulence: our forced results better replicate observed ocean turbulence statistics than did prior unforced simulations of decaying coherent vortices. Both in simulations and in ocean observations, the transverse velocity gradients show tails that decay more slowly than Gaussian pdfs, but substantially faster than Cauchy pdfs. In forced two-dimensional turbulence the longitudinal and transverse gradient pdfs differ. This difference is surprising in light of previous results for the case of three-dimensional turbulence [22] as well as the unforced two-dimensional case [2] which lead to similar results in both the transverse and longitudinal directions. Further study of forced two-dimensional turbulence appears likely to shed light on oceanic processes.

Acknowledgments. The work of N.S. was supported by a grant from the Research Grants Council of the Hong Kong Special Administrative Region, China (RGC Ref. No. CUHK4119/98P) and by a postdoctoral fellowship from the Chinese University of Hong Kong. S.T.G. was supported by NASA through the Jason Altimeter Science Working Team (JPL contract 1204910).

References

- [1] A. S. Monin and A. M. Yaglom. *Statistical Fluid Mechanics*. MIT Press, Cambridge, Massachusetts, 1975.
- [2] J. Jimenez. Algebraic probability density tails in decaying isotropic two-dimensional turbulence. *J. Fluid Mech.*, 313:223, 1996.
- [3] I. A. Min, I. Mezic, and A. Leonard. Levy stable distributions for velocity and velocity differences in systems of vortex elements. *Phys. Fluids*, 8:1169, 1996.
- [4] C. Wunsch and D. Stammer. Satellite altimetry, the marine geoid, and the oceanic general circulation. *Annu. Rev. Earth Planet. Sci.*, 26:219, 1998.
- [5] P. B. Rhines. Geostrophic turbulence. *Annu. Rev. Fluid Mech.*, 11:401, 1979.
- [6] J. C. McWilliams. The emergence of isolated coherent vortices in turbulent flow. *J. Fluid Mech.*, 146:21, 1984.

- [7] W. G. Large, W. R. Holland, and J. C. Evans. Quasi-geostrophic ocean response to real wind forcing—the effects of temporal smoothing. *J. Phys. Oceanogr.*, 21:998, 1991.
- [8] C. K. Wikle, R. F. Miliff, and W. G. Large. Surface wind variability on spatial scales from 1 to 1000 km observed during TOGA COARE. *J. Atmos. Sci.*, 56:2222, 1999.
- [9] N. Schorghofer. Universality of probability distributions among two-dimensional turbulent flows. *Phys. Rev. E*, 61:6568, 2000.
- [10] N. Schorghofer. Energy spectra of steady two-dimensional turbulent flows. *Phys. Rev. E*, 61:6572, 2000.
- [11] S. G. Llewellyn Smith and S. T. Gille. Probability density functions of large-scale turbulence in the ocean. *Phys. Rev. Lett.*, 81:5249, 1998.
- [12] S. T. Gille and S. G. Llewellyn Smith. Velocity probability density functions from altimetry. *J. Phys. Oceanogr.*, 30:125, 2000.
- [13] A. Bracco, J. H. LaCasce, and A. Provenzale. Velocity probability density function for oceanic floats. *J. Phys. Oceanogr.*, 30:461, 2000.
- [14] H. Takahashi and T. Gotoh. Small-scale statistics in two-dimensional turbulence. *Proc. Res. Inst. Math. Sci. (Kyoto Univ.)*, 972:163, 1996.
- [15] B. N. Kuvshinov and T. J. Shep. Holtsmark distributions in point-vortex systems. *Phys. Rev. Lett.*, 84:650, 2000.
- [16] P. H. Chavanis and C. Sire. The statistics of velocity fluctuations arising from a random distribution of point vortices: the speed of fluctuations and the diffusion coefficient. Preprint, 2000.
- [17] G. L. Mellor. *Introduction to Physical Oceanography*. Springer-Verlag, New York, 1996.
- [18] S. Kida and Y. Murakami. Statistics of velocity gradients in turbulence at moderate reynolds numbers. *Fluid Dyn. Res.*, 4:347, 1989.
- [19] A. Vincent and M. Meneguzzi. The spatial structure and statistical properties of homogeneous turbulence. *J. Fluid Mech.*, 225:1, 1991.
- [20] S. Chen, G. D. Doolen, R. H. Kraichnan, and Z. S. She. On statistical correlations between velocity increments and locally averaged dissipation on homogeneous turbulence. *Phys. Fluids A*, 5:458, 1993.

- [21] K. Yamamoto and T. Kambe. Gaussian and near-exponential probability-distributions of turbulence obtained from a numerical simulation. *Fluid Dyn. Res.*, 8:65, 1991.
- [22] U. Frisch and Z. S. She. On the probability density-function of velocity-gradients in fully-developed turbulence. *Fluid Dyn. Res.*, 8:139, 1991.
- [23] F. Belin, J. Maurer, P. Tabeling, and H. Willaime. Velocity gradient distributions in fully developed turbulence: An experimental study. *Phys. Fluids*, 9:3843, 1997.
- [24] H. S. Shafi, Y. Zhu, and R. A. Antonia. Statistics of partial derivative u_y in a turbulence wake. *Fluid Dyn. Res.*, 19:169, 1997.
- [25] R. H. Kraichnan. Models of intermittency in hydrodynamic turbulence. *Phys. Rev. Lett.*, 65:575, 1990.
- [26] R. Benzi, L. Biferale, G. Paladin, A. Vulpiani, and M. Vergassola. Multifractality in the statistics of the velocity gradients in turbulence. *Phys. Rev. Lett.*, 67:2299, 1991.
- [27] G. K. Batchelor. *The Theory of Homogeneous Turbulence*. Cambridge University Press, Cambridge, 1953.
- [28] L.J.M Kroon and N.J. Bink. Conditional statistics of vertical heat fluxes in local advection conditions. *Boundary-Layer Met.*, 80:49, 1996.
- [29] E. S. C. Ching. General formula for stationary or statistically homogeneous probability density functions. *Phys. Rev. E*, 53:5899, 1996.
- [30] N. Takahashi, T. Kambe, T. Nakano, T. Gotoh, and K. Yamamoto. Probability density function of longitudinal velocity increment in homogeneous turbulence. *J. Phys. Soc. Japan*, 68:86, 1999.

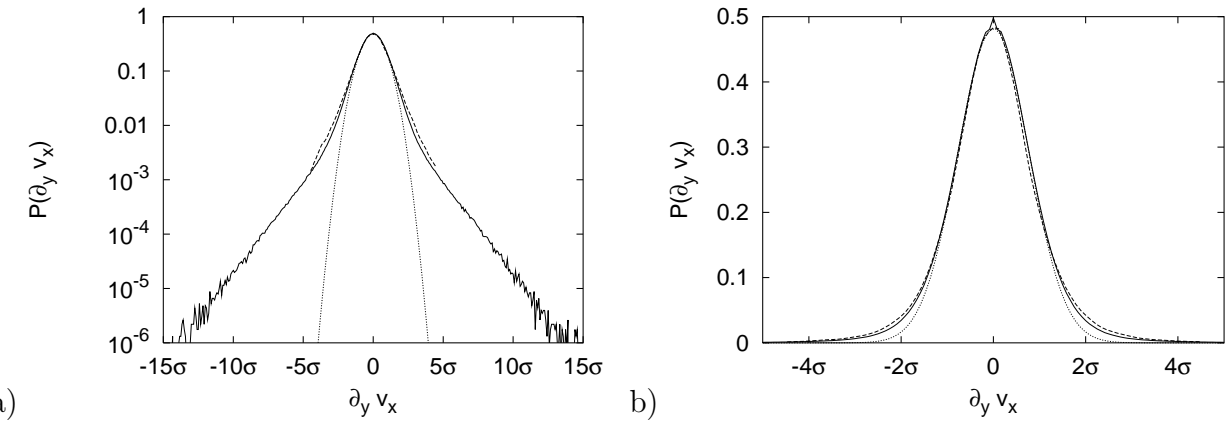


Figure 1: (a) Global variance-normalized pdf of the velocity gradient in the ocean (solid line) compared with simulations of two-dimensional Navier-Stokes turbulence (dashed line) on a semi-logarithmic scale. (b) Same quantities on a linear scale. In both cases, a fitted Gaussian is shown for comparison (dotted line). The difference in the length of the tails reflects the enormous difference in Reynolds numbers. The ocean pdf is averaged over about 13 million data points. Data are normalized by the standard deviations $\sigma = \sqrt{\langle (\partial_y v_x)^2 \rangle}$, as described in the text.

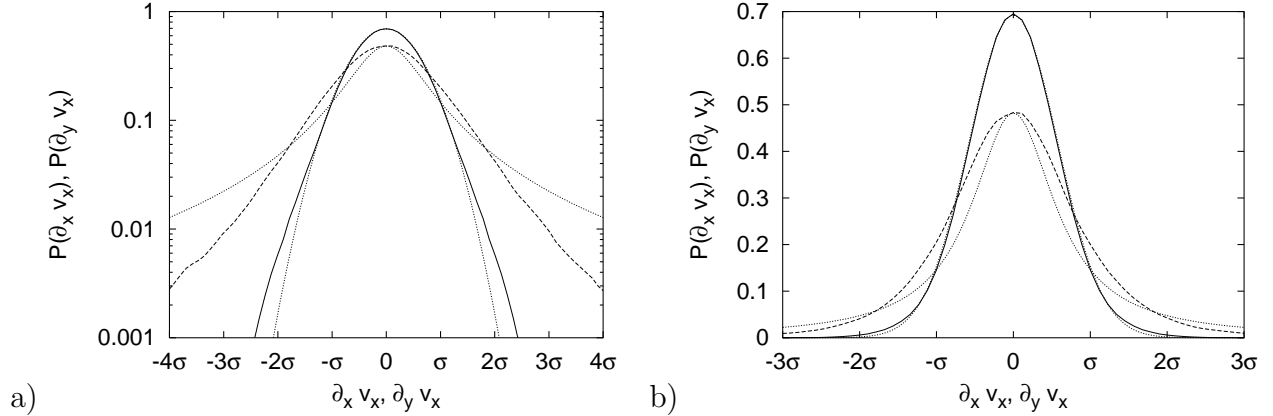


Figure 2: (a) Probability density functions of velocity derivatives for forced two-dimensional Navier-Stokes turbulence on a semi-logarithmic scale. (b) Same quantities on a linear scale. In both panels, the dashed line shows the transverse component, $\partial_y v_x$, and the solid line the longitudinal component, $\partial_x v_x$. Both are normalized by the standard deviation of the transverse component $\sigma = \sqrt{\langle (\partial_y v_x)^2 \rangle}$. The two dotted lines are a Gaussian and a Cauchy distribution respectively. Transversal and longitudinal gradient pdf differ from each other in width and shape.

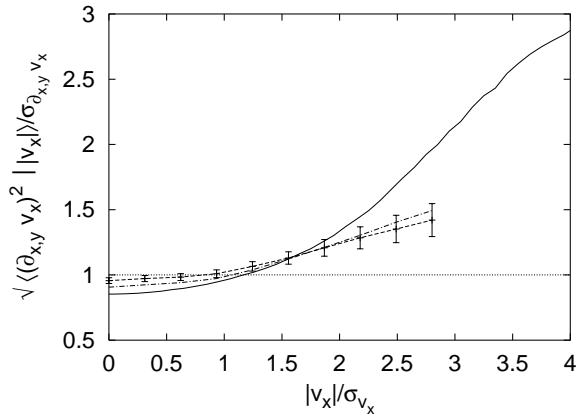


Figure 3: Conditional average of transverse velocity gradient with velocity, $\sqrt{\langle (\partial_y v_x)^2 | v_x | \rangle}$, for two-dimensional Navier-Stokes (dashed line with error bars) and ocean turbulence (solid line). The dash-dot line shows the longitudinal component, $\sqrt{\langle (\partial_x v_x)^2 | v_x | \rangle}$, in the Navier-Stokes simulation. All three graphs are normalized by their respective standard deviation. The error bars include only the statistical error expected from averaging of the 32 snapshots, showing twice the standard error of the mean.